ANL-06/52

Argonne NATIONAL LABORATORY

Thermal-fluid and Electrochemical Modeling and Performance Study of a Planar Solid Oxide Electrolysis Cell: Analysis on SOEC Resistances, Size, and Inlet Flow Conditions

Nuclear Engineering Division

About Argonne National Laboratory

Argonne is a U.S. Department of Energy laboratory managed by UChicago Argonne, LLC under contract DE-AC02-06CH11357. The Laboratory's main facility is outside Chicago, at 9700 South Cass Avenue, Argonne, Illinois 60439. For information about Argonne, see www.anl.gov.

Availability of This Report

This report is available, at no cost, at http://www.osti.gov/bridge. It is also available on paper to the U.S. Department of Energy and its contractors, for a processing fee, from:

U.S. Department of Energy
Office of Scientific and Technical Information
P.O. Box 62
Oak Ridge, TN 37831-0062
phone (865) 576-8401
fax (865) 576-5728
reports@adonis.osti.gov

ANL-06/52

Thermal-fluid and Electrochemical Modeling and Performance Study of a Planar Solid Oxide Electrolysis Cell: Analysis on SOEC Resistances, Size, and Inlet Flow Conditions

by
B. Yildiz, J. Smith, and T. Sofu
Nuclear Engineering Division, Argonne National Laboratory

June 30, 2006

Abstract

Argonne National Laboratory and Idaho National Laboratory researchers are analyzing the electrochemical and thermal-fluid behavior of solid oxide electrolysis cells (SOECs) for high temperature steam electrolysis using computational fluid dynamics (CFD) techniques. The major challenges facing commercialization of steam electrolysis technology are related to efficiency, cost, and durability of the SOECs. The goal of this effort is to guide the design and optimization of performance for high temperature electrolysis (HTE) systems.

An SOEC module developed by FLUENT Inc. as part of their general CFD code was used for the SOEC analysis by INL. ANL has developed an independent SOEC model that combines the governing electrochemical mechanisms based on first principals to the heat transfer and fluid dynamics in the operation of SOECs. The ANL model was embedded into the commercial STAR-CD CFD software, and is being used for the analysis of SOECs by ANL.

The FY06 analysis performed by ANL and reported here covered the influence of electrochemical properties, SOEC component resistances and their contributing factors, SOEC size and inlet flow conditions, and SOEC flow configurations on the efficiency and expected durability of these systems. Some of the important findings from the ANL analysis are:

1) Increasing the inlet mass flux while going to larger cells can be a compromise to overcome increasing thermal and current density gradients while increasing the cell size. This approach could be beneficial for the economics of the SOECs;

2) The presence of excess hydrogen at the SOEC inlet to avoid Ni degradation can result in a sizeable decrease in the process efficiency;

3) A parallel-flow geometry for SOEC operation (if such a thing be achieved without sealing problems) yields smaller temperature gradients and current density gradients across the cell, which is favorable for the durability of the cells;

4) Contact resistances can significantly influence the total cell resistance and cell temperatures over a large range of operating potentials. Thus it is important to identify and avoid SOEC stack conditions leading to such high resistances due to poor contacts.

THERMAL-FLUID AND ELECTROCHEMICAL MODELING AND PERFORMANCE STUDY OF A PLANAR SOLID OXIDE ELECTROLYSIS CELL:

Analysis on SOEC Resistances, Size, and Inlet Flow Conditions

Bilge Yildiz, Jeff Smith, Tanju Sofu

June 30, 2006

Argonne National Laboratory, Nuclear Engineering Division,

9700 S Cass Avenue, Bldg 208, Argonne, IL 60439

byildiz@anl.gov, tsofu@anl.gov

INTRODUCTION

The analysis reported here covers the influence of the electrochemical properties, the solid oxide electrolysis cell (SOEC) resistances and their contributing factors, the SOEC size and inlet flow conditions, and SOEC flow configurations on the efficiency and expected durability of these systems. The analysis is performed by using the SOEC electrochemical and thermal-fluid model developed at ANL as a module to the STAR-CD Computational Fluid Dynamics software.

High temperature steam electrolysis (HTE) is an environmentally acceptable and effective candidate process for hydrogen production in evolving hydrogen markets. The currently considered HTE system concepts and demonstrations are based on solid oxide electrolysis cells (SOECs) that are similar to those used for solid oxide fuel cells (SOFCs)[1],[2]. The major challenges in front of the commercialization of this technology are related to the cost and durability of the SOECs with high efficiency in operation. The goal of this project is to develop and utilize a model that can guide the performance optimization of high temperature electrolysis (HTE) systems.

The SOECs operate with an applied potential to electro-catalytically split steam into $H_{2(g)}$ and $O_{2(g)}$. There is limited knowledge about the intermediate reaction steps that define the phenomenological behavior of solid oxide electro-chemistry, especially for the less investigated SOEC mode of operation. Only limited studies existed concerning the SOECs priorly. The model developed in this work at ANL[3] appropriately combines the governing electrochemical mechanisms based on the first-principals to the heat transfer and fluid dynamics in the operation of SOECs. In this way, it is used to guide the design and optimization of SOEC-based hydrogen production systems, as well as to allow the detailed investigation

of the SOEC performance. In addition, this model can be coupled to a complete simulation model of the full-size HTE plant to support the plant thermodynamic analysis.

THERMAL-FLUID AND ELECTROCHEMICAL MODEL

The model has been developed to simulate a planar 3-dimentional SOEC by using a finite element approach. The model combines an in-house developed electrochemical (EC) module and the commercially available computational fluid dynamics (CFD) code STAR-CD. It calculates the local electrochemical kinetics of the SOEC coupled to the mass- and heat-balances of the gaseous flow and the solid medium. The main coupling between the EC and CFD modules is due to the mutual use of the temperature profile. The CFD module provides the temperature field for the EC module to generate the current density distribution through using the temperature dependent electrochemical parameters. The EC module provides the species and heat generation rates, based on the current density that it calculates, for the CFD module to generate the consistent temperature profile. The details of the electrochemical model embedded to the combined EC-CFD model for this analysis was provided in the FY05 Report on this task and is found in Ref. [3].

The CFD module, based on the STAR-CD code, performs thermal and flow analysis with the specified boundary conditions, and the heat and species generation rates calculated by the EC module. The flow in the porous electrode and flow-mesh regions of the SOEC is modeled as a compressible multi-component mixture with relevant heat and mass sources and sinks. The details of the CFD code STAR-CD can be found from Ref. [4].

SIMULATIONS

A planar square geometry SOEC with cross flow configuration is considered in this study as the initial application, representative of the SOECs being demonstrated for steam electrolysis in DOE's NHI-HTSE program. The geometric parameters and material properties of the electrolyte-supported cell-stack currently being tested at Idaho National Laboratory (INL) make part of the input to the simulations. The schematic for the cross-flow configuration of the SOEC is shown in Figure 1. The electrolyte, the oxygen electrode (anode), and hydrogen electrode (cathode) are made of scandia stabilized zirconia (YSZ), composite of perovskite and doped-fluorite, and Ni-SSZ cermet, respectively. The hydrogen electrode has a mixture of steam, hydrogen and an inert carrier-gas of nitrogen at 800^{o}C and atmospheric pressure at its inlet. The total flow rate and mass fraction of hydrogen and nitrogen at the cathode inlet is varied as a parameter in our simulations. The oxygen electrode has air at 800^{o}C and atmospheric pressure at its inlet. A list of major input parameters of the model is given in the Table I.

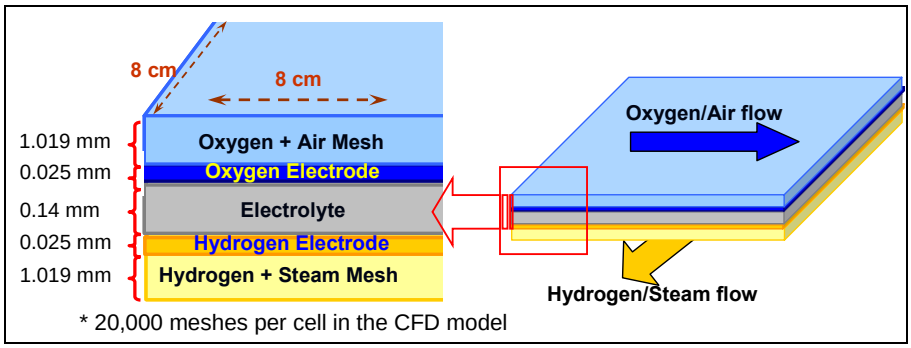

Figure 1: The schematic for the cross-flow configuration of SOEC used as the base case in the simulations (not-to-scale).

Table I: Model input parameters for the base case geometry and flow conditions

Geometry parameters	
Active cell width (m)	8×10^{-2}
Anode (oxygen electrode) thickness (m)	2.5×10^{-5}
Cathode (hydrogen electrode) thickness (m)	2.5×10^{-5}
Electrolyte thickness (m)	1.4×10^{-4}
H_2- and O_2-flow channel thickness (m)	1.019×10^{-3}
Material properties (at 1073 ^{o}K)	
Specific resistivity of anode (Ωm)	1.425×10^{-4}
Specific resistivity of cathode (Ωm)	8.856×10^{-6}
Specific resistivity of electrolyte (Ωm)	$1.07 \times 10^{-4} \exp(7237/T)$
Specific resistivity of O_2-flow channel (Ωm)	1.176×10^{-6}
Specific resistivity of H_2-flow channel (Ωm)	1.176×10^{-6}
Thermal conductivity of anode (W/mK)	9.6
Thermal conductivity of cathode (W/mK)	1.31×10^{1}
Thermal conductivity of electrolyte (W/mK)	2.16
Thermal conductivity of O_2-flow channel (W/mK)	1.6×10^{1}
Thermal conductivity of H_2-flow channel (W/mK)	7.2×10^{1}
Activation polarization	
Exchange current density parametric range for the anode (A/m2)	1300 – 4000
Diffusion polarization	
Porosity of anode and cathode (%)	37
Porosity of flow-meshes (%)	87
Tortuosity of anode and cathode	3.0
Permeability of anode (m^{-2}) (isotrpic)	1×10^{-13}
Permeability of cathode (m^{-2}) (isotropic)	1×10^{-13}
Permeability of flow channel (m^{-2})	
In the flow direction	2×10^{-4}
Perpendicular to the flow direction	2×10^{-5}
Ohmic polarization	
Material resistivities given under the “Material properties”	--

Electrolyte resistivity

The analysis in our FY05 study has assumed the electrolyte to be made of yttria-stabilized zirconia (YSZ). In FY06, we have updated our model for electrolyte properties to represent the scandia stabilized zirconia (SSZ) consistently with the materials being tested at INL SOEC experiments. SSZ conductivity is 3-5 times better than YSZ conductivity at 973-1273 K, as shown in Figure 2. All the analysis performed in FY06 analysis (partially reported here) included the SSZ properties.

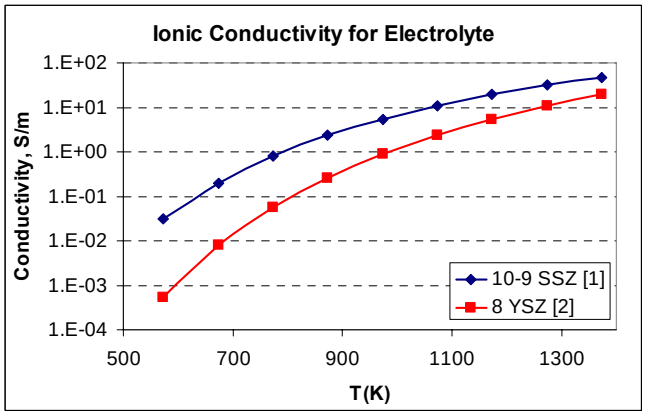

ρ_{SSZ} (Ω.m)= 1.07E-4xexp(7237/T) Ref: **[5]**
ρ_{YSZ} (Ω.m) = 3.69E-4+ 2.84E-5 exp(10300/T) Ref: [6]

Figure 2: Ionic conductivity for the YSZ and SSZ electrolyte material as a function of temperature

Simulations were performed with the above stated operating conditions for a range of applied cell-potential values in order to determine the cell efficiency, and temperature and current distribution profiles.

The following major assumptions were taken for the simulations:

- Steady-state conditions,
- Uniform potential distribution at the outer boundary of the electrodes and interconnects, i.e. equipotential electrode and interconnect surfaces.
- Adiabatic boundary conditions at the top and bottom surfaces of the cell. i.e. representative of a cell inside a stack.
- Heat exchange by radiation in actual operation is negligible.

The last assumption reflects the hypothesis of modeling a cell which is considered to be packed with similar cells / stacks on all sides inside a canister of many cells/stacks, so that the net external radiation effects may be neglected.

RESULTS AND DISCUSSION

The model of the representative SOEC as shown in Figure 1 uses 12 layers of elements: 4 layers in each flow mesh, 1 layer in each electrode and 2 layers in the electrode. The planar area of the cell layers is divided into 40x40 elements for the base case of 8cmx8cm active cell area. The number of elements is varied for comparative case runs proportional with the size of the cells. Thus, the complete cell in the finite element model for the base case is comprised of 19200 elements. The sensitivity of results with respect to further fineness in the discretization of the cell is negligible with the given number of elements per cell.

The influence of several parameters on the resulting efficiency, temperature and current density profiles is investigated. The conditions that were varied for this purpose are the electrochemical properties (oxygen electrode exchange current density, and contact resistance), SOEC size, hydrogen mass fraction at the cathode inlet, steam and air flow rates at the SOEC inlets, and flow configuration (cross-flow, and parallel-flow). For each case, the polarization behavior of the simulated cell is studied within the applied cell potential of 0.8–1.6V.

Electrochemical properties

Exchange current density

The exchange current density, i_o, is related to the activation of the electrode intermediate reactions that control the performance of the electrode at lower current densities. It depends on the material catalytic activity, temperature and partial pressure of the reacting species that is oxygen in our case. Although it has been widely studied, the details of the O_2-electrode reactions and the form of the exchange current density have not been clearly understood[7] as stated in the section for the electrochemical model description.

The model incorporates the dependence of i_o upon these changing variables within the cell. The P_{O2} and temperature dependence of i_o for oxygen reduction reaction can be expressed as in Equation 1. Since we do not have more detailed kinetic data about oxygen evolution reaction on SOEC electrodes, first, we assume a similar form of dependence as in Equation 1 for the i_o relevant SOEC anodes for the present model. When data is retrieved for SOEC anode kinetics for specified materials, a more appropriate model for i_o can be implemented in the model.

$$i_o = \gamma_{electrode}\left(\frac{P_{O_2}}{P_{total}}\right)^{0.25} e^{\left(-\frac{E_{act}}{RT}\right)} \quad (1)$$

Experimental data[8] showing a relation between the cell temperature and exchange current density for the LSM-YSZ composite cathode for SOFC was compared with reported ranges of γ and E_{act}, to produce a close fit. By using a γ of $7x10^8$ A/m^2 and activation energy (E_{act}) of 115 kJ/mol, the calculated exchange current density approximates the experimental data closely, as shown in Figure 3. At 800C, the i_o value for a composite electrode as in Figure 3 is 1300 A/m^2.

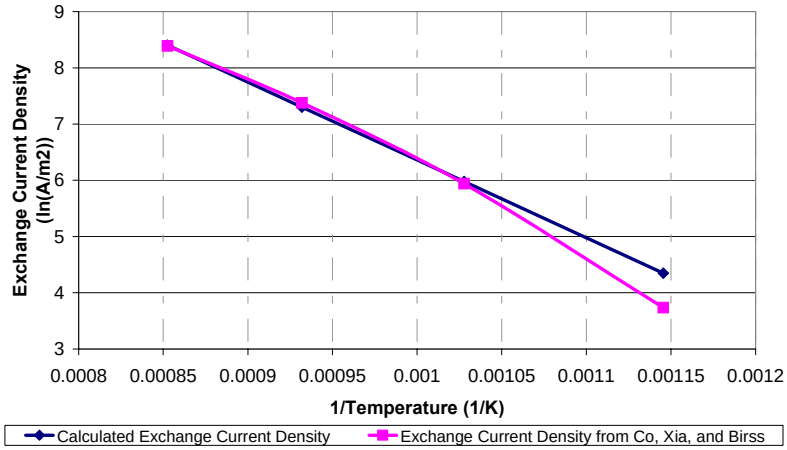

Figure 3: Experimental versus calculated temperature dependant exchange current density with E_{act} set at 115 kJ/mol.

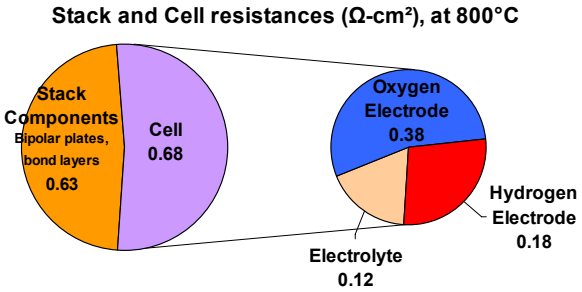

Stack data courtesy of Ceramatec (J. Hartvigsen)
Single cell data courtesy of INL (J. O'Brien)

Figure 4: Polarization contributors for INL SOEC Experiments

The oxygen electrode ASR in the SOEC cells was determined to be 0.38 Ωcm^2 by Ceramatec and INL measurements (Figure 4), which would require an exchange current density of 1225A/m^2. This value is consistent with the predicted and measured results shown in Figure 3. However, the prior simulations of ANL and INL on SOECs have shown to include i_o as 4000A/m^2, which compared well to the INL SOEC stack measurements. Nevertheless, the difference imposed on the results (shown for polarizarion (Figure 5-a), cell ASR(Figure 5-b) and cell temperature (Figure 5-c)) due to the variation in the exchange current density (from 1300 to 3500 A/m^2) is significant. *Therefore, a more thorough analysis of this parameter,*

using both experiments and simulations, is needed in order to obtain a quantitatively precise set of results from the model predictions in the future.

Although the range of i_o covered here is consistent with the relevant data for LSM in literature for different designs, the influence on the change of polarization behavior is noteworthy. *It emphasizes the importance of the knowledge necessary about the oxygen electrode phenomena for the modeling to help the electrode design in a more precise way.*

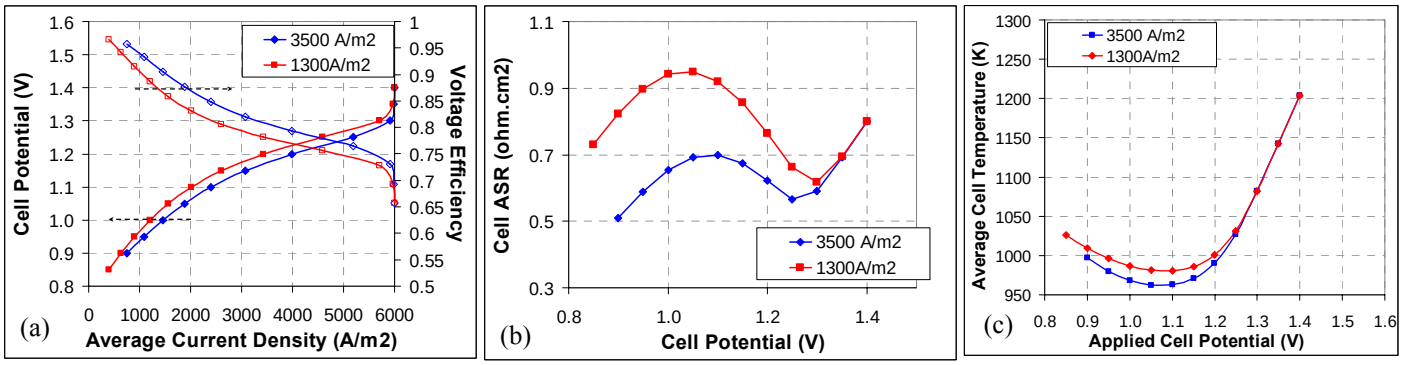

Figure 5: Effect of the oxygen electrode exchange current density on the (a) polarization and voltage efficiency, (b) average Nernst potential, and (c) average cell temperature in the SOEC.

Contact resistance

The contact resistances can play an important role in the performance of the SOECs. They govern the resistances at the interface of the electrode/flow-mesh, and flow-mesh/interconnect plates, when the SOECs are made into stacks. The difference between the button cell ASR (~0.7 ohm.cm^2) and the stack ASR (~2.8 ohm.cm^2 from INL's SOEC stack experiments[9] in 08/2005) indicate a high interfacial resistance due to these contacts (~2 ohm.cm^2). With typical material properties of the SOEC active components as shown in Table I, the operation with 2ohm.cm^2-contact resistance can yield severe losses at the SOEC output as compared to the case with no contact resistances. For example, for an applied potential of 1.3V per cell, the output can decrease from 6000A/m^2 to 2000A/m^2, that is equivalently a 60% loss in output of hydrogen (Figure 6). *The influence of the contact resistances on total cell ASR and on cell temperature is significant over a large range of operating potentials as seen in Figure 6-a-c and comprises a large fraction of the cell ASR. It important to identify and evade the SOEC stack conditions leading to such high resistances due to contacts.*

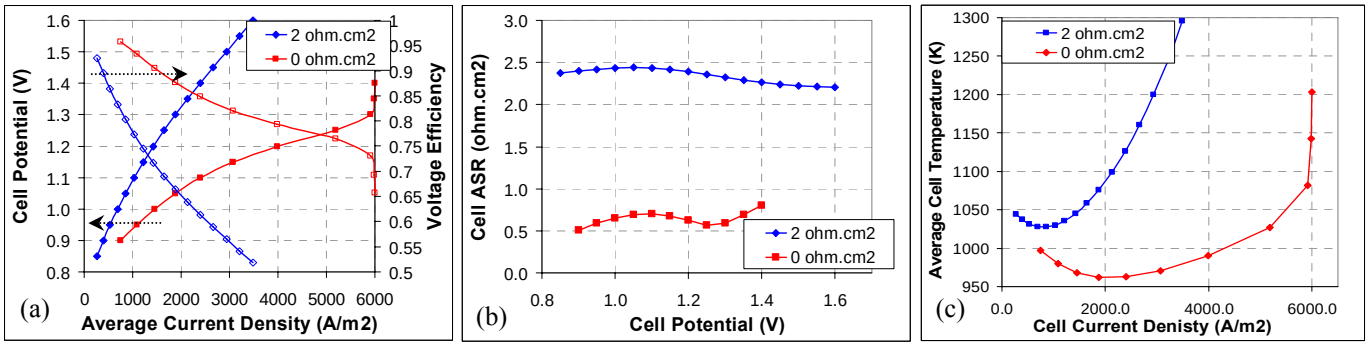

Figure 6: Effect of the contact resistance on the (a) polarization and voltage efficiency, (b) total cell ASR, and (c) average cell temperature in the SOEC.

Comparison to INL data and Cell ASR components

A comparison of the simulated and the measured polarization results was performed. The closest results are obtained using the temperature and P_{O2} dependent expression of Io, as in Eq.1, with a value of 4000A/m2 at 800C, 7 mol% of H2 mass fraction at the inlet, 50mol% mass fraction of N2 at the inlet, and 1 ohm.cm^2 of contact resistances, as shown in Figure 7-a. For this case, the resulting variation of temperature and Io as a function of cell potential for an adiabatic cell is shown in Figure 7-b.

Case B:
$H_{2,inlet}$ = 7 mol%
Io_{800C} = 4000A/m2
R_{int} = 1 ohm.cm2

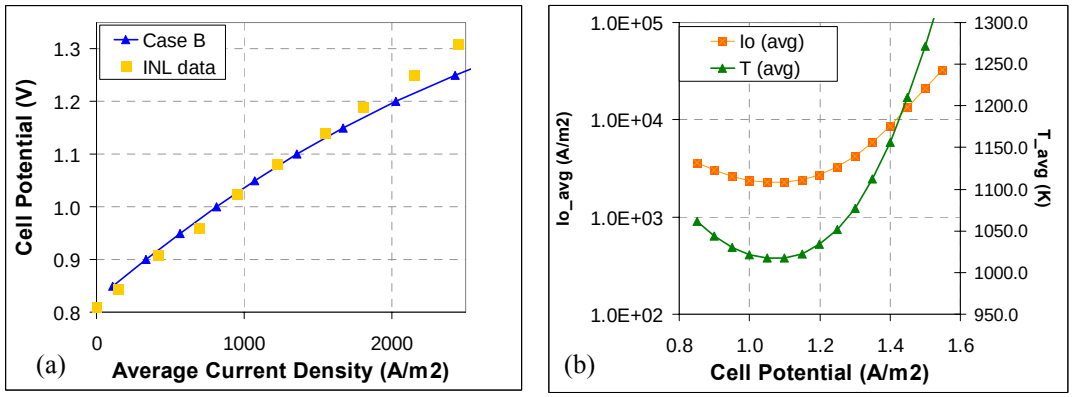

Figure 7: (a) Polarization, (b) Average cell temperature and exchange current density in the SOEC.

The contributors to the cell ASR are the ohmic resistances (from the electrolyte, electrodes, the flow-meshes, and the contacts), the activation component (from the anode) and the diffusion component (from the cathode). The major contributors to the ohmic resistances are the electrolyte and the contact resistance, and the resistance of the electrodes and flow meshes (metal components) is negligible. The decomposition of the ASR components are shown in Figure 8–A and –B for a 1300A/m^2 and 4000A/m^2 of I_o value, respectively. The contact resistance, oxygen electrode, and electrolyte are, respectively, the

largest contributors to the cell ASR in Case A. The contact resistance is the major cause for the high cell ASR in Case B, where the oxygen electrode is better (with a higher exhange burrent density. i.e faster oxygen exhange rate) than in Case A, and and has approxiamtely equal resistance as the the electrolyte. *Under these representative conditions, the foremost contributor to the cell ASR is the contact resistances, followed by the oxygen electrode (anode) and the electrolyte.*

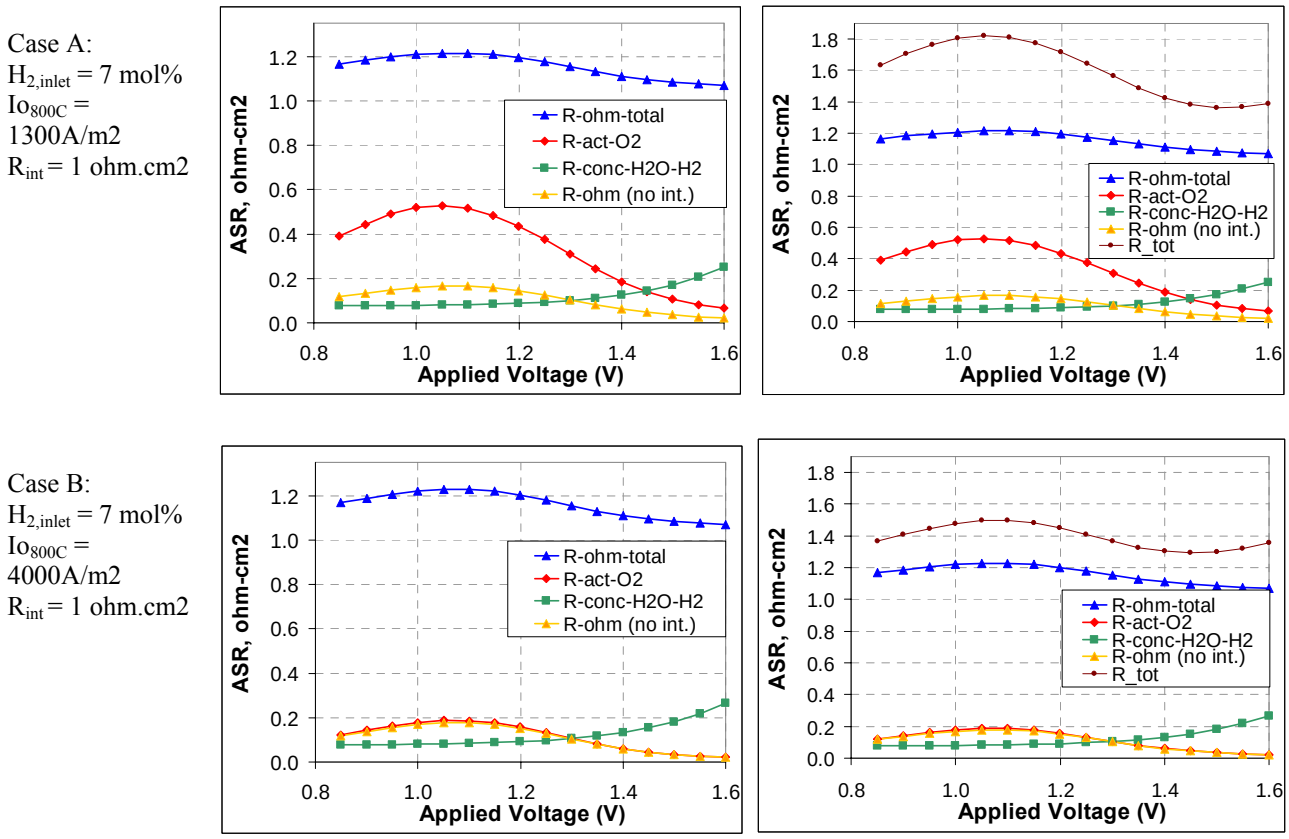

Figure 8: (A-1,-2) Cell ASR components for Case A, (B-1,-2) Cell ASR components for Case B

SOEC lateral size

The lateral size, thus the area per cell, of the SOECs influences the total size of an HTSE plant, thus the capital cost. The larger cells per one unit of and HTSE plant can eliminate the auxiliary equipment needed per unit output from the plant, and thus reduce the overall size of the plant for a given power rate. However, the SOEC size influences the cell polarization, and cell temperature, as well as the hydrogen output rate. The size-effect on electrochemical polarization and on cell temperature is shown for a 4cmx4cm, a 8cmx8cm (the base case cell) and a 16cmx16cm SOEC, in Figure 9-a and -b. In these simulations, the thickness of the flow meshes, the cell components and the mass flux at the steam and air

inlets are kept the same. The smaller size cells (e.g. 4cmx4cm) yield a higher current density, thus, higher efficiency, although the difference is relatively small. On the other hand, the influence of SEOC size on the temperature and current density is more pronounced below and above the thermal neutral potential (i.e. 1.3V for 800°C at the inlets). Although the SOECs being tested at INL currently operate at the thermal neutral potential (1.3V), an actual HTSE plant may operate below or above 1.3V to maximize the thermal efficiency of the hydrogen plant. *The results show that the temperature and current density profiles have less steep gradients at smaller cell sizes below and above the thermal neutral potential.* The simulation results are shown for the three cell sizes in Figure 10 for 1.2V and in Figure 11 for 1.4V. The large thermal gradients impose stresses that can lead to mechanical failure of the cells, and the large current density gradients can lead to SOEC materials performance degradation due to non-uniform utilization of materials under electrical field. These results indicates that, *even if the larger SOECs can be more economical from the capital cost point of view, the larger temperature and current density gradients are not favorable in terms of efficiency and durability.* Therefore, if the inlet mass flux of the SOEC is kept the same, the choice for the cell size must be a compromise between the capital cost, the efficiency, and durability of the SOEC materials.

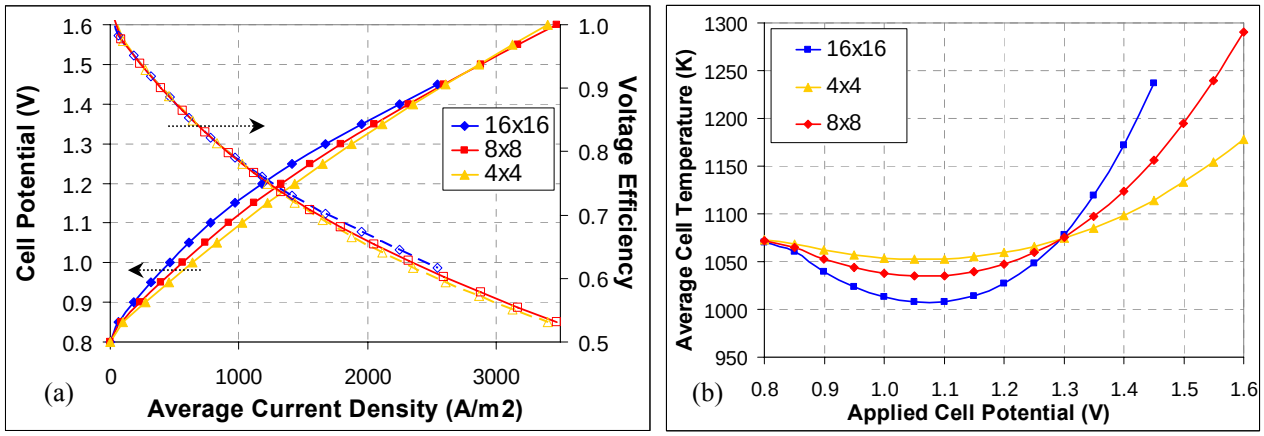

Figure 9: Effect of the SOEC cell width (4cmx4cm, 8cmx8cm, 16cmx16cm) on (a) polarization and voltage efficiency, (b) average cell temperature in the SOEC.

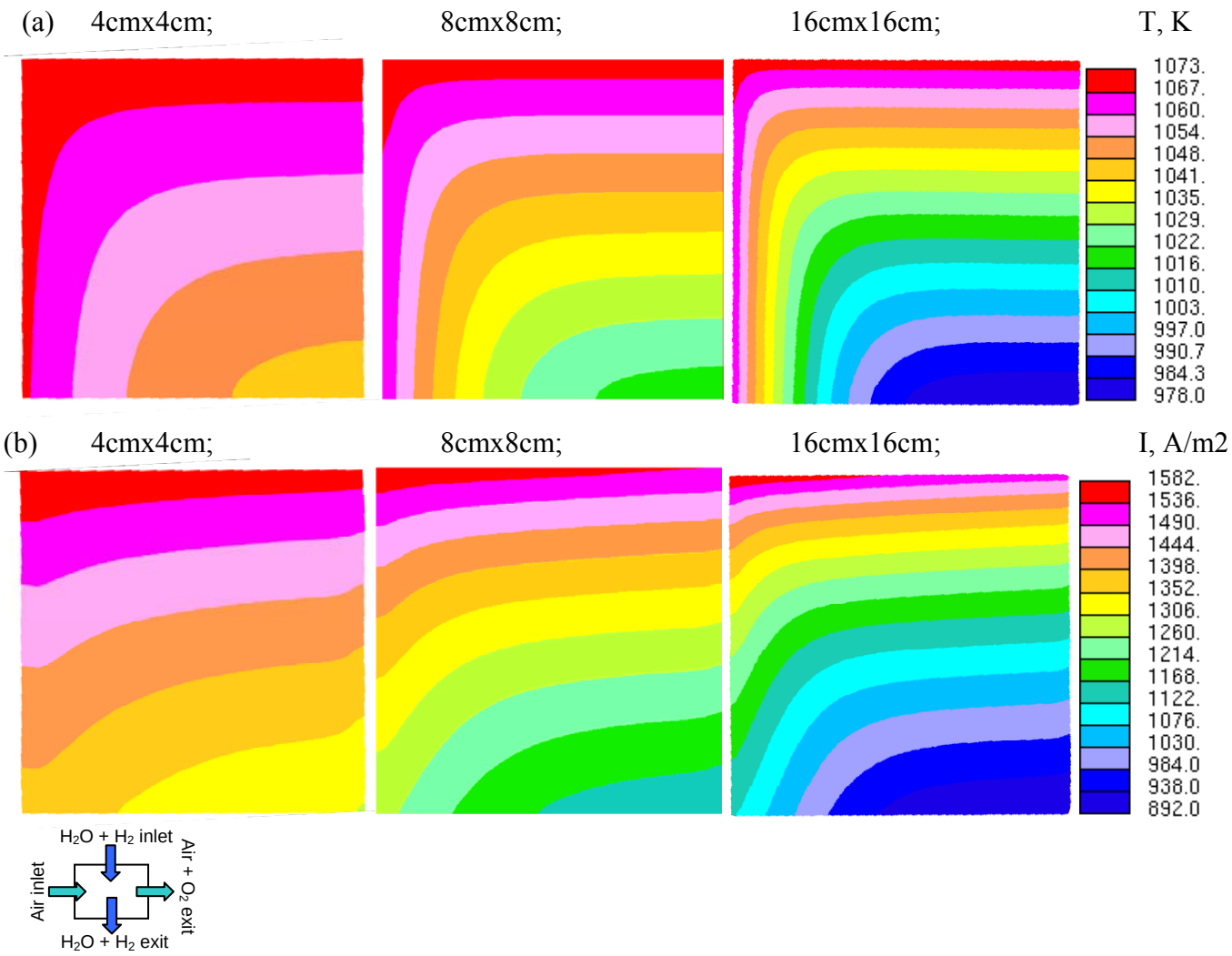

Figure 10: Simulated profiles of (a) temperature, K, (b) current density, A/m2, for V_{appl} = 1.2V

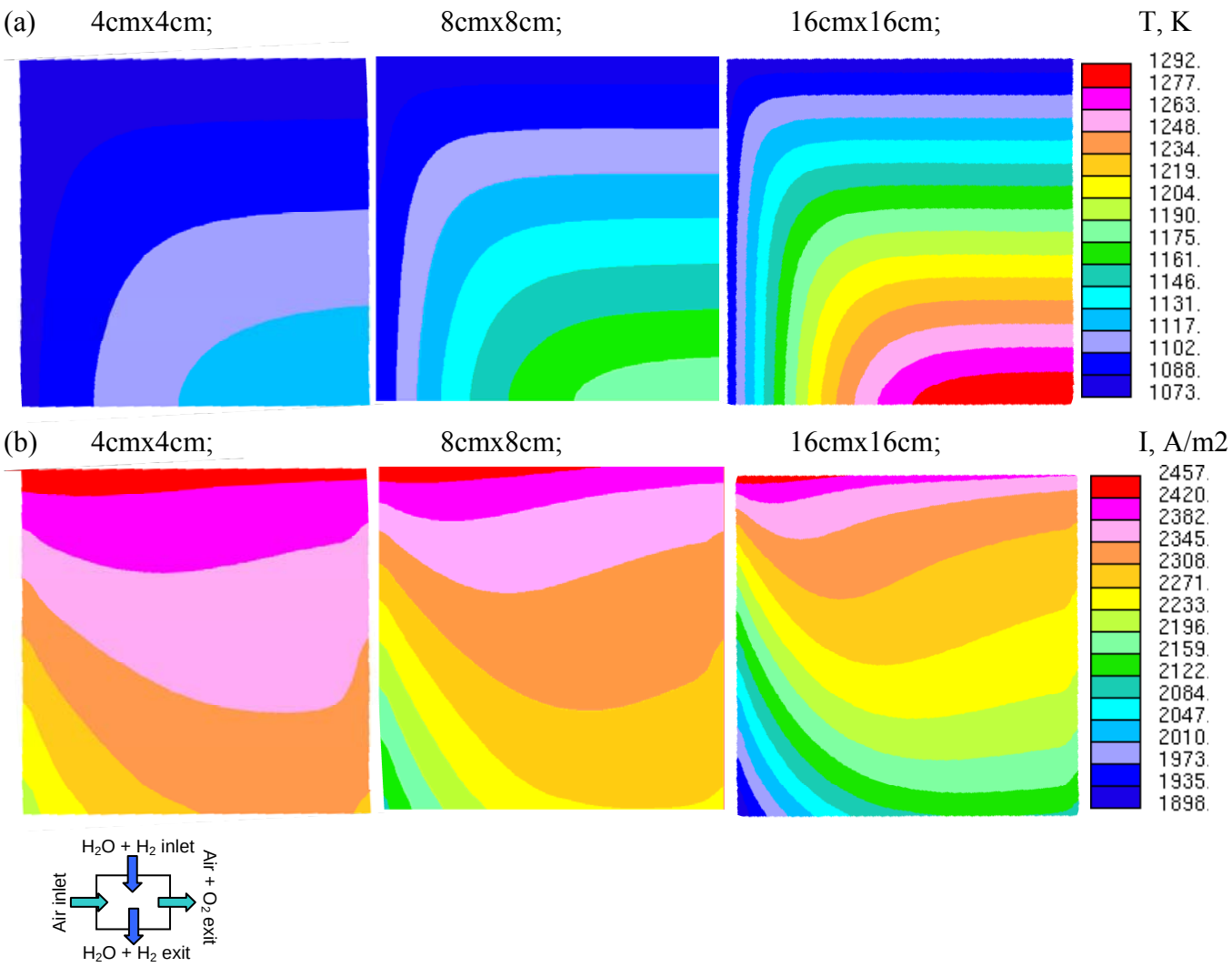

Figure 11: Simulated profiles of (a) temperature, K, (b) current density, A/m2, for V_{appl} = 1.4V

Cathode inlet flow conditions

Flow rate

For a given cell size, the flow rate of steam and air was also varied to understand its influence on the cell performance. This influence is studied on an 8cmx8cm cell by keeping the flow mesh thickness the same. Therefore an increase in the in flow rate implies a proportional increase in the inlet mass flux. Consistently with the results for the size-effect (above), the increase in the flow rate at the inlets increases the current density output rate of the cell, as shown in Figure 12. The gradients in the temperature and current density profile, for below and above 1.3V, decrease when the SOEC inlet flow rate is increased. Therefore, if the cells can be well sustained mechanically under high flow conditions, *operating the SOEC with higher flow rates can be favorable both in terms of efficiency and in terms of the durability of the cells. Increasing the inlet mass flux while going to larger cells can be a compromise to overcome the increasing thermal and current density gradients while increasing the cell size, and be beneficial for the economics of the SOECs.*

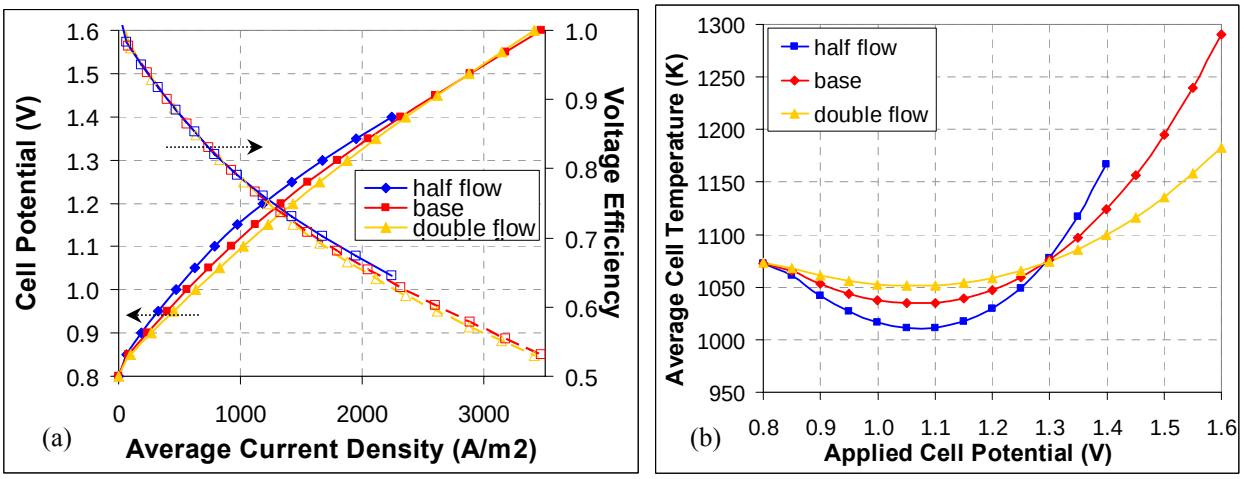

Figure 12: Effect of the SOEC inlet mass flux (half, base, double) on (a) polarization and voltage efficiency, (b) average cell temperature in the SOEC.

Hydrogen and Nitrogen mass fraction at the cathode inlet

Hydrogen can be desirable at the inlet of the SOEC cathode to avoid the oxidation related degradation of the Ni catalyst in the Ni-YSZ electrode. The influence of excess hydrogen, for 800°C and 1atm, at the cathode inlet is shown in Figure 13. Excess hydrogen in the cathode leads to increased cell potential required at a given current density at operation, mainly due to an increased Nernst potential in the presence of excess H_2. *When the mass fraction of hydrogen is increased from 0 to 10 and to 50mol%, the resulting additional electrical potential requirement is about 4% and 15% of* LHV_{H2}. This effect can

notably degrade the overall process efficiency. Nevertheless, the presence of excess hydrogen in cathode can help extend the durability of the SOECs although it decreases the overall efficiency of the process. Therefore, either a cathode with oxidation resistance under SOEC conditions must be developed, or a compromise between the process efficiency and cell durability must be found in deciding for the mass fraction of H2 at the steam-inlet of SOEC.

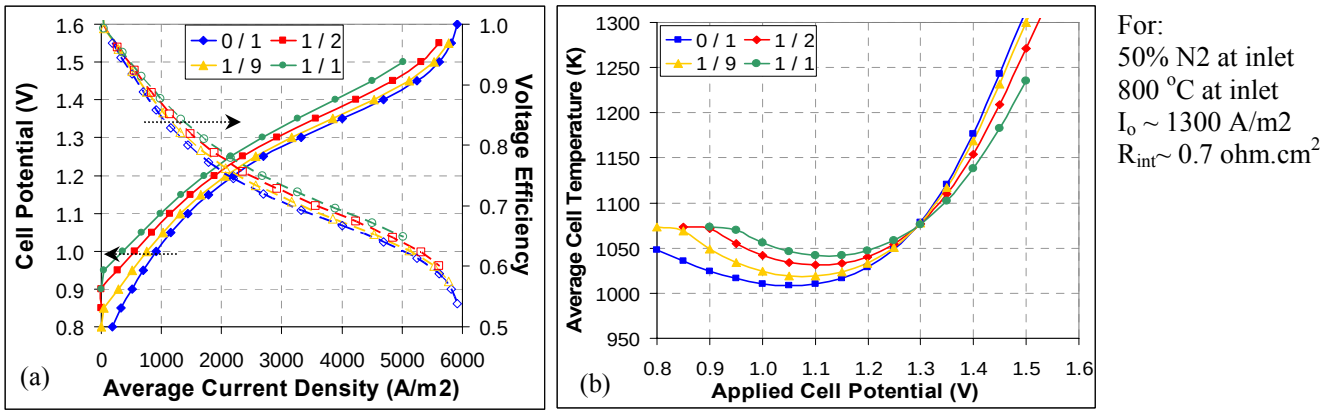

For:
50% N2 at inlet
800 °C at inlet
I_o ~ 1300 A/m2
R_{int}~ 0.7 ohm.cm^2

Figure 13: Effect of the presence of excess hydrogen (in mol fraction ratio) *(H_2/H_2O)* at the cathode on the (a) polarization and voltage efficiency, (b) average cell temperature in the SOEC.

Flow inlet configuration

The cross flow configuration of the flow paths, as shown in Figure 1, has been the conventional scheme for both the SOFC and SOEC mode of operation due to the ease of separating the product streams from each other in a stack.

The calculated voltage efficiency in these simulations is comparable to those typical of SOFC operation. The temperature differential across the cell is minimized (i.e. no thermal gradients) at the thermal neutral potential of the SOEC. Nevertheless, as the applied potential (and consequently the current density) increases, the temperature gradients and the difference between the maximum and the minimum temperatures in the cell increase[3]. Operating the SOECs with large thermal gradients is not a desirable condition, though thermal gradients can be minimized through cell design to operate below or above the V_{tn} to optimize the HTSE efficiency. Severe thermal gradients can cause thermal stresses and degradation of the SOEC materials and the durability of the system. This effect emphasizes *the importance of simulations for performance optimization because operating at higher current density at or above the thermal neutral point with very small temperature gradient can significantly improve the efficiency, durability and cost of the SOEC system.* The simulations indicate that comparable electrochemical polarization at the same cell potential, $V_{applied}$, can be attained with different flow configurations, but the

temperature profiles can be considerably different. Figure 14 show a set of examples to this finding. Almost the same current density and voltage efficiency can be can be achieved at the given values of $V_{applied}$ for the cross- and parallel-flow configurations, as presented in Figure 14. Nevertheless, *the parallel-flow SOEC (if achievable in practice) yields lower temperature gradients across the cell, which is favorable for the durability of the cells. The difference is more significant for higher values of* $V_{applied}$ *and current density,* as presented in Figure 15. Similarly, although an average same current density can be achieved in cross- and parallel flow configurations, the current density distribution, thus the utilization of steam across the cell can vary differently, as shown in Figure 16.

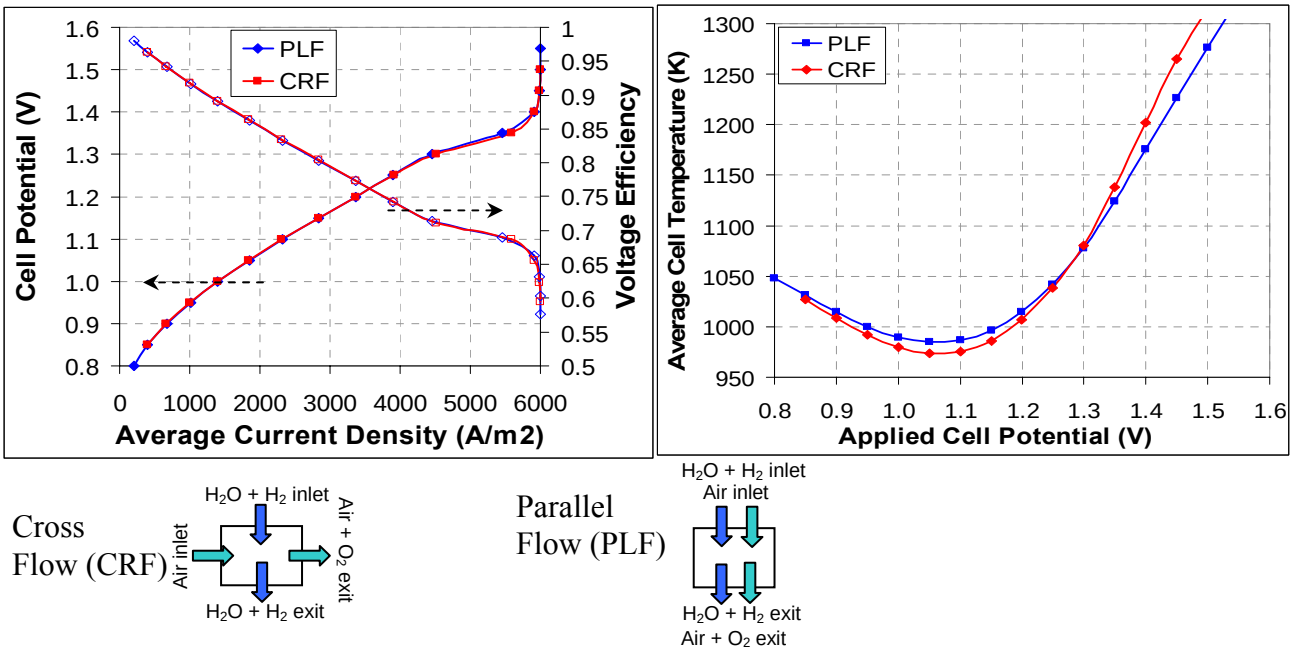

Figure 14: Simulated results of (a) polarization and voltage efficiency, and (b) average cell temperature for the cross-flow and parallel-flow configuration SOEC. Inlet conditions: 800°C and 1atm, with 0% mass fraction of H_2 and 50% mass fraction of N_2 at the cathode inlet.

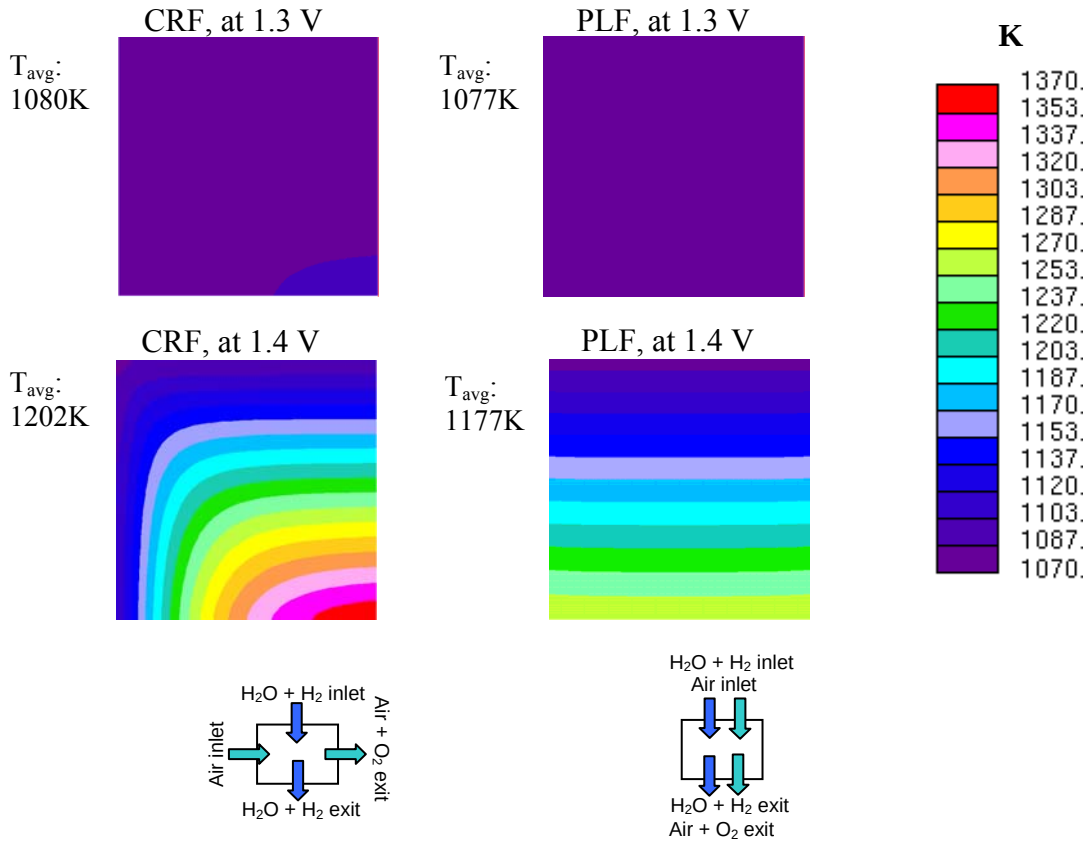

Figure 15: Simulated profiles of SOEC temperature for cross-flow (CRF) and parallel flow (PLF) SOEC configuration with $V_{applied}$:1.3V and 1.4V. Inlet conditions: 800^{o}C and 1atm.

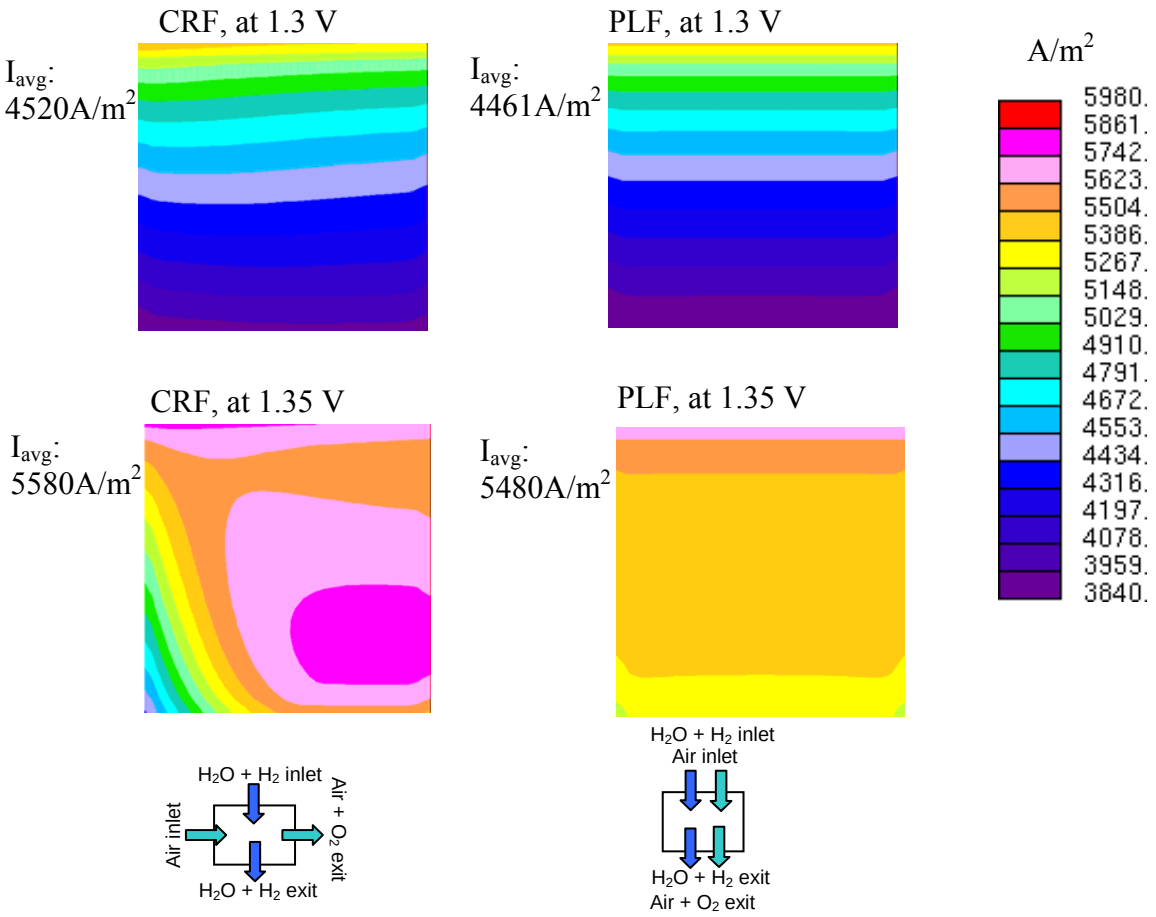

Figure 16: Simulated profiles of SOEC current density for cross-flow (CRF) and parallel flow (PLF) SOEC configuration with $V_{applied}$:1.3V and 1.35V. Inlet conditions: 800^{o}C and 1atm.

Base Case Variations

The conditions summarized in Table II were simulated as base case comparisons with INL modeling studies. Some of the results are shown in Figure 17 and will be compared with INL results in the next phases of our project.

Table II: Case definitions for base case model runs.

Parameter	**Case 1**	**Case 2**
Mass flow rate cathode	8.0e-6 kg/s	15.0e-6 kg/s
Mass flow rate anode	4.0e-6 kg/s	4.0e-6 kg/s
Mass fractions cathode	N2 = 0.50, H2O = 0.493902, H2 = 0.006098	N2 = 0.50, H2O = 0.493902, H2 = 0.006098
Mass fractions anode	O2 = 0.23, N2 = 0.77	O2 = 0.23, N2 = 0.77
Operating pressure	101.325 kPa	101.325 kPa
Inlet temperature	1073 K	1073 K
Exchange current density	10^{20} A/m2	4000 A/m^2
Electrolyte resistivity	0.5 Ω-m	0.1 Ω-m
Contact resistance	0 Ω-m^2	10^{-4} Ω-m^2

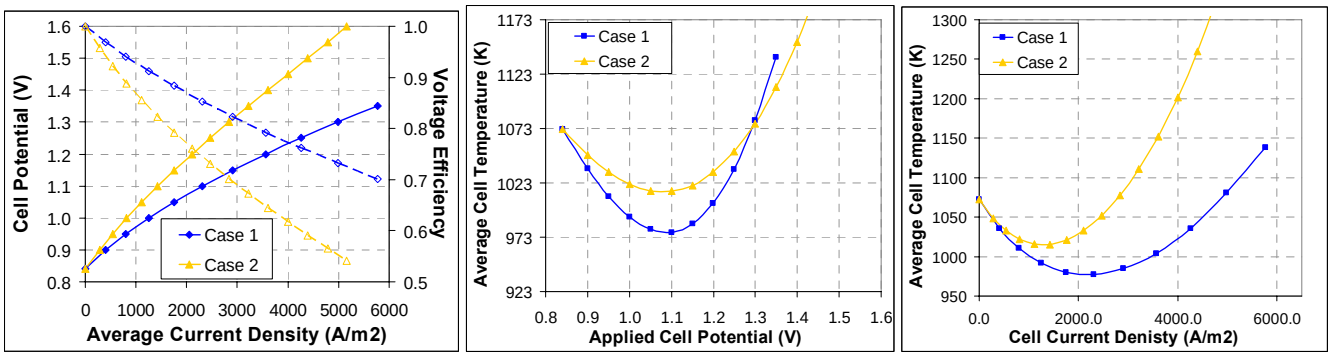

Figure 17: Effect of the contact resistance on the (a) polarization and voltage efficiency, (b,c) average cell temperature in the SOEC.

CONCLUDING REMARKS AND FUTURE WORK

The current simulations do not represent a geometry and flow configuration that minimizes the temperature and current density gradients, but are demonstrations of the framework for the capability to predict the coupled electrochemical and CFD behavior of the HTE system. Qualitative comparisons of results with respect to electrochemical properties, size and flow conditions and configuration of the SOECs are presented in this report. The ultimate objective in the progress of this work is to identify the operating cell and stack flow configurations that can optimize the temperature distribution while maintaining a good hydrogen production performance of the HTSE system.

The model developed in this work at ANL is unique with the capability to couple SOEC specific electrochemical behavior to the transport processes based on the first-principals of the governing electrochemical mechanisms. There is yet uncertainty about specifically the reaction activation related phenomena for both the SOFC and SOEC electrodes. Thus, further findings in that area can help improve the mechanism definition in the model presented here. Such an integrated simulation capability can also help eliminate the mechanism related uncertainties that can arise due to using an SOFC specific model with parametric modifications for SOECs. The major differences between the SOFC and SOEC operation of the same cell materials are the reaction activation for catalytic reactions and the thermal behavior due to energetics of the overall reaction. The former can be accommodated in this work by including several possible kinetic models for reaction activation controlling mechanism. One of these kinetic models with temperature and partial pressure dependence is already encoded into the SOEC model.

The results from the model in this work indicate the large margin for improving the performance of the SOECs. Our main concluding remarks from this analysis are as follows:

- A more thorough analysis of the *oxygen electrode electrochemical properties*, using both experiments and simulations, is needed in order to obtain a quantitatively precise set of results from the model predictions in the future.
- The contact resistances, oxygen electrode activation, and electrolyte resistance are, respectively, the *largest contributors to the cell initial ASR.*
- *Contact resistances* can significantly influence the total cell ASR and cell temperature over a large range of operating potentials, and they can comprise a large fraction of the cell ASR. It important to identify and evade the SOEC stack conditions leading to such high resistances due to contacts.
- The temperature and current density profiles have less steep gradients at *smaller cell sizes* below and above the thermal neutral potential. These results indicates that, even if the larger SOECs can be more

economical from the capital cost point of view, the larger temperature and current density gradients are not favorable in terms of efficiency and durability.

- Operating the SOEC with *higher flow rates* can be favorable both in terms of efficiency and in terms of the durability of the cells, if the SOEC can be well sustained mechanically under high flow conditions. *Increasing the inlet mass flux while going to larger cells can be a compromise to overcome the increasing thermal and current density gradients while increasing the cell size, and be beneficial for the economics of the SOECs.*
- When the mass fraction of *hydrogen at SOEC inlet* is increased to avoid Ni degradation, the resulting additional *electrical potential requirement* is significant. Therefore, either a cathode with oxidation resistance under SOEC conditions must be developed, or a compromise between the process efficiency and cell durability must be found in deciding for the mass fraction of H2 at the steam-inlet of SOEC.
- The *parallel-flow SOEC* (if achievable in practice) yields lower temperature gradients and current density gradients across the cell, which is favorable for the durability of the cells. The difference is more significant for higher values of $V_{applied}$ and current density.

In future work, for more detailed validation of the SOEC model, the simulation results will be compared to the SOEC polarization, flow and temperature related measurements performed at INL. The comparison of the model results to experiments should assist to reduce the uncertainty of various assumptions on different key model parameters. The model will also be extended to other flow configurations and SOEC designs to compare their performance to the base case cross- and parallel-flow configurations. The *Tuff-Cell* design of ANL is one of the primary candidates that can imitate the parallel-flow with smaller temperature gradients, and it is subject to investigation with this model. The electrochemical efficiency and uniformity of temperature distribution within the cells will be the major performance parameters for the comparison of the cell and stack configurations.

ACKNOWLEDGEMENTS

This work was financially supported by the U.S. Department of Energy, Office of Technology Support Programs, under Contract Number W-31-109-ENG-38 and by the Office of Nuclear Energy, Science and Technology. We thank Drs. Steve Herring, James O'Brein, Carl Stoots and Grant Hawkes from Idaho National Laboratory for providing us with the necessary details of the operating conditions and some properties of the SOEC tests for our simulations and for useful discussions with them about the modeling results.

REFERENCES

[1] R. Hino, K. Haga, H. Aida, K. Sekita, *Nuclear Engineering and Design,* 233, 233 (2004).

[2] J. E. O'Brein, C. M. Stoots, J. S. Herring, J. Hartvigsen, *in FUELCELL2005 Proceedings, Third International Conference on Fuel Cell Science and Technology* (2005).

[3] B. Yildiz, T. Sofu, *FY05 Report for DOE* on Thermal-fluid and Electrochemical Modeling and Performance Study of a Planar Solid Oxide Electrolysis Cell.

[4] http://www.cd-adapco.com/

[5] O. Yamamoto, *Electrochimica Acta* 45 (2000)

[6] D. Herbstrit, *The Electrochemical Society, PV* 2001-16 (2001)

[7] S. B. Adler, *Chemical Reviews*, 104, 4791 (2004).

[8] A. Co, S. Jiang Xia, V. I. Birss, *Journal of the Electrochemical Society,* 152, A570-A576, (2005).

[9] J.E. O'Brien, C.M. Stoots, J.S. Herring, Documentation of INL High-Temperature Electrolysis Milestone Demonstrating 100 NL/hr Hydrogen Production Rate, August 1, 2005.

Nuclear Engineering Division
Argonne National Laboratory
9700 South Cass Avenue, Bldg. 208
Argonne, IL 60439-4842

www.anl.gov

UChicago ▶ Argonne LLC

A U.S. Department of Energy laboratory
managed by UChicago Argonne, LLC